Nuclear Mathematical and Computational Sciences: A Century in Review, A Century Anew
Gatlinburg, Tennessee, April 6-11, 2003, on CD-ROM, American Nuclear Society, LaGrange Park, IL (2003)

MAXIMUM PRINCIPLE ANALYSIS OF MONTE CARLO METHODS FOR GREY RADIATIVE TRANSFER

Jeffery D. Densmore
Transport Methods Group CCS-4
Los Alamos National Laboratory
Los Alamos, NM 87545
jdensmor@engin.umich.edu

Edward W. Larsen
Department of Nuclear Engineering and Radiological Sciences
University of Michigan
Ann Arbor, MI 48109
edlarsen@engin.umich.edu

ABSTRACT

Exact solutions of radiative transfer problems have been proven to satisfy a maximum principle. In this paper we show that solutions to grey (frequency-independent) radiative transfer problems generated by the Carter-Forest Monte Carlo method are guaranteed to satisfy the maximum principle for sufficiently small time steps, but may violate it for large time steps. We then compare a similar analysis of the Fleck-Cummings Monte Carlo method to ours. We demonstrate that the Fleck-Cummings method is guaranteed to satisfy the maximum principle for larger time steps than the Carter-Forest method. We also present numerical simulations in which one or both Monte Carlo methods violate the maximum principle.

Key Words: radiative transfer, Monte Carlo, maximum principle

1. INTRODUCTION

In radiative transfer problems, photons are born at a radiation source and transport stochastically through the problem medium until they are absorbed or escape from the system. When a photon is absorbed, its energy is deposited in the material, which increases the material temperature. Due to temperature-dependent Planckian emission, the material itself is a source of photons [7].

Radiative transfer problems are inherently nonlinear and time dependent. Not only is the Planckian source a function of temperature, but so is the opacity, which determines the mean free path of photons, and the heat capacity, which relates material energy and temperature. These nonlinearities cause difficulties when simulating radiative transfer problems.

Several Monte Carlo methods exist for solving radiative transfer problems. These methods linearize the problem within each time step by using the beginning of step values for both the opacity and heat capacity, then solve the linearized problem using a standard Monte Carlo simulation. However, these methods treat photon absorption, increase in material energy and temperature, and subsequent photon emission within the time step in an implicit manner. These Monte Carlo methods differ in their implicit approximation of this absorption-reemission process. In the Fleck-Cummings method [4], this process is approximated by

including additional scattering into the transport simulation. The Carter-Forest method [2] models the correct absorption-reemission process, in which photons are absorbed and then reemitted at a later time. However, the Carter-Forest method is still an approximation, since the parameters that govern the absorption-reemission process are evaluated at explicit temperatures.

Since the Carter-Forest method models the physical absorption-reemission process more closely than the Fleck-Cummings method, one may expect the Carter-Forest method to produce solutions with less truncation error than the Fleck-Cummings method, at least if the error introduced by the linearization process is ignored. However, radiative transfer problems are nonlinear and explicit approximations are present in both methods. Thus, it is possible that both methods will demonstrate unphysical behavior for sufficiently large time steps. It is not clear to what extent unphysical behavior is experienced or what constraints on the time-step size are required to avoid unphysical solutions by simply examining how each method models the absorption-reemission process.

Radiative transfer problems have been shown to satisfy a maximum principle [1] [6]. This principle guarantees that the exact solutions of radiative transfer problems are bounded by the initial and boundary conditions. It is desirable to know if the above Monte Carlo methods satisfy the maximum principle, and if so, under what constraints. Larsen and Mercier [5] have shown that "ideal" solutions obtained using the Fleck-Cummings method are guaranteed to satisfy the maximum principle for sufficiently small time steps, but may experience unphysical behavior for large time steps. (By ideal solutions, we mean solutions to the underlying linearized equations that are free from statistical error, not the results from a specific Monte Carlo simulation.) In this paper, we perform an analysis, similar to that of Larsen and Mercier's, for the Carter-Forest method in the case of grey (frequency-independent) radiative transfer. As with the Fleck-Cummings method, we show that ideal solutions generated by the Carter-Forest method are guaranteed to satisfy the maximum principle for sufficiently small time steps, but may violate it for large time steps. In addition, we demonstrate that the Fleck-Cummings method is guaranteed to satisfy the maximum principle for larger time steps than the Carter-Forest method. This implies that the Carter-Forest method is less stable than the Fleck-Cummings method.

We begin the remainder of this paper with a description of the equations of radiative transfer, and the maximum principle which they satisfy. Next, we develop both the Fleck-Cummings and Carter-Forest Monte Carlo methods. We then perform a maximum principle analysis for the Carter-Forest method, which determines constraints on the time-step size that guarantees the maximum principle is satisfied. This analysis of the Carter-Forest method is then compared to that of the Fleck-Cummings method. Finally, we present numerical results for both methods.

2. PROBLEM DESCRIPTION

We begin by presenting the equations of grey (frequency-independent) radiative transfer. In the absence of internal sources and scattering, these equations are [7]

$$\frac{1}{c}\frac{\partial I}{\partial t} + \mathbf{\Omega}\cdot\nabla I = \sigma\left(\frac{1}{4\pi}acT^4 - I\right) \quad , \tag{1}$$

and

$$\frac{\partial U_m}{\partial t} = \sigma\left(\int I d\Omega - acT^4\right) \quad , \tag{2}$$

where $I(\mathbf{r}, \mathbf{\Omega}, t)$ is the radiation intensity and $T(\mathbf{r}, t)$ is the material temperature. In addition, $\sigma(\mathbf{r}, T)$ is the opacity, a is the radiation constant, and c is the speed of light. We have assumed local thermodynamic equilibrium such that the Planckian emission source is given by

$$\frac{1}{4\pi}\sigma acT^4 \quad . \tag{3}$$

The material energy density, $U_m(T)$, and material temperature are related by

$$\frac{\partial U_m}{\partial T} = C_v > 0 \quad , \tag{4}$$

where $C_v(\mathbf{r}, T)$ is the heat capacity. In Eqs. (1) and (2), $\mathbf{r} \in D$ represents the spatial variable, $\mathbf{\Omega} \in 4\pi$ represents the angular variable, and $t > 0$ represents the time variable.

In addition to Eqs. (1) and (2), we require initial conditions that specify I and T for $t = 0$:

$$I(\mathbf{r}, \mathbf{\Omega}, 0) = I_i(\mathbf{r}, \mathbf{\Omega}) \quad , \tag{5}$$

$$T(\mathbf{r}, 0) = T_i(\mathbf{r}) \quad , \tag{6}$$

and a boundary condition that specifies I on the outer boundary of the system ($\mathbf{r} \in \partial D$) for incoming directions ($\mathbf{\Omega} \cdot \mathbf{n} < 0$, where $\mathbf{n}$ is the unit outward normal vector on ∂D):

$$I(\mathbf{r}, \mathbf{\Omega}, t) = I_b(\mathbf{r}, \mathbf{\Omega}, t) \quad . \tag{7}$$

The equations of radiative transfer are known to satisfy the following maximum principle [1] [6]:

Maximum Principle. Let $0 \leq T_L < T_U$ be fixed constants, and let I_i, T_i, and I_b satisfy

$$\frac{1}{4\pi}acT_L^4 \leq I_i(\mathbf{r}, \mathbf{\Omega}) \leq \frac{1}{4\pi}acT_U^4 \quad , \tag{8}$$

$$T_L \leq T_i(\mathbf{r}) \leq T_U \quad , \tag{9}$$

and

$$\frac{1}{4\pi}acT_L^4 \leq I_b(\mathbf{r}, \mathbf{\Omega}, t) \leq \frac{1}{4\pi}acT_U^4 \quad , \quad \mathbf{r} \in \partial D \quad , \quad \mathbf{\Omega} \cdot \mathbf{n} < 0 \quad . \tag{10}$$

Then, for all $\mathbf{r} \in D$, $\mathbf{\Omega} \in 4\pi$, and $t > 0$,

$$\frac{1}{4\pi}acT_L^4 \leq I(\mathbf{r}, \mathbf{\Omega}, t) \leq \frac{1}{4\pi}acT_U^4 \quad , \tag{11}$$

and

$$T_L \leq T(\mathbf{r}, t) \leq T_U \quad . \tag{12}$$

In other words, if a problem has initial and boundary conditions that lie between two Planckians, then the solution forever lies between these two Planckians.

3. OVERVIEW OF MONTE CARLO METHODS

To develop a Monte Carlo method for radiative transfer, we must first linearize Eqs. (1) and (2). We begin by defining the equilibrium radiation energy density as

$$U_r(T) = aT^4 \quad . \tag{13}$$

Next, we rewrite the left hand side of Eq. (2) as

$$\frac{\partial U_m}{\partial t} = \frac{\partial U_m}{\partial T}\frac{\partial T}{\partial U_r}\frac{\partial U_r}{\partial t} = \frac{1}{\beta}\frac{\partial U_r}{\partial t} \quad , \tag{14}$$

where, employing Eqs. (4) and (13),

$$\beta = \frac{\partial T}{\partial U_m}\frac{\partial U_r}{\partial T} = \frac{4aT^3}{C_v} \quad . \tag{15}$$

Then, using Eqs. (13) and (14), Eqs. (1) and (2) become

$$\frac{1}{c}\frac{\partial I}{\partial t} + \mathbf{\Omega}\cdot\nabla I = \sigma\left(\frac{1}{4\pi}cU_r - I\right) \quad , \tag{16}$$

$$\frac{1}{\beta}\frac{\partial U_r}{\partial t} = \sigma\left(\int I d\Omega - cU_r\right) \quad . \tag{17}$$

The nonlinear terms in Eqs. (16) and (17) now consist of only σ and β.

Next, we subdivide the problem into a series of time steps $0 = t_0 < t_1 < t_2 < \cdots$. Then, for $t_n \le t \le t_{n+1}$, we approximate σ and β by their beginning of time step values:

$$\beta(\mathbf{r}, T) \approx \beta(\mathbf{r}, T_n) = \beta_n(\mathbf{r}) \quad , \tag{18}$$

$$\sigma(\mathbf{r}, T) \approx \sigma(\mathbf{r}, T_n) = \sigma_n(\mathbf{r}) \quad , \tag{19}$$

where $T_n(\mathbf{r}) = T(\mathbf{r}, t_n)$ is the material temperature at the beginning of the time step. In practice, σ and β may also be evaluated at an extrapolated temperature within the time step. However, in this paper we consider only explicit approximations of σ and β. With this linearization, Eqs. (16) and (17) can be approximated for $t_n \le t \le t_{n+1}$ as

$$\frac{1}{c}\frac{\partial I}{\partial t} + \mathbf{\Omega}\cdot\nabla I = \sigma_n\left(\frac{1}{4\pi}cU_r - I\right) \quad , \tag{20}$$

and

$$\frac{1}{\beta_n}\frac{\partial U_r}{\partial t} = \sigma_n\left(\int I d\Omega - cU_r\right) \quad . \tag{21}$$

Eqs. (20) and (21) now represent two coupled, linear equations. The boundary condition for Eq. (20) is provided by Eq. (7), and the initial conditions for Eqs. (20) and (21) are given by the previous time step, or by Eqs. (5) and (6) if $n = 0$.

To implement Eqs. (20) and (21) into a Monte Carlo method, Eq. (21) is used to approximate U_r within the time step. This approximation is then employed in Eq. (20), which can then be solved using a standard Monte Carlo simulation. At the end of the time step, the Monte Carlo-calculated radiation intensity and the approximated version of U_r are substituted into Eq. (2) to calculate the new material energy density. Using

Eq. (19) to approximate the opacity, and integrating over the nth time step, Eq. (2) gives the end of time-step material energy density as

$$U_m(T_{n+1}) = U_m(T_n) + \sigma_n \int_{t_n}^{t_{n+1}} \left(\int I d\Omega - cU_r \right) dt \quad . \tag{22}$$

Eq. (4) can then be solved to determine the temperature at the beginning of the next time step, T_{n+1}.

The Fleck-Cummings and Carter-Forest methods differ in their treatment of Eq. (21) and their approximation to U_r. We now outline both of these methods.

3.1. The Fleck-Cummings Method

To derive the Fleck-Cummings method [4], we begin by integrating Eq. (21) over the nth time step. This yields

$$U_r(T_{n+1}) = U_r(T_n) + \sigma_n \beta_n \int_{t_n}^{t_{n+1}} \left(\int I d\Omega - cU_r \right) dt \quad . \tag{23}$$

Next, we approximate the step-averaged value of U_r by interpolating between the beginning and end of time-step values,

$$\frac{1}{\Delta t_n} \int_{t_n}^{t_{n+1}} U_r dt = \tilde{U}_r = \alpha U_r(T_{n+1}) + (1-\alpha) U_r(T_n) \quad , \tag{24}$$

where $\Delta t_n = t_{n+1} - t_n$. In Eq. (24), α is a parameter chosen by the user, and is usually between 1/2 and 1. Using Eqs. (23) and (24), the value of U_r at the end of the time step is

$$U_r(T_{n+1}) = \frac{1}{1+\alpha\beta_n c\sigma_n \Delta t_n} \left\{ [1-(1-\alpha)\beta_n c\sigma_n \Delta t_n] U_r(T_n) + \beta_n \sigma_n \int_{t_n}^{t_{n+1}} \int I(\mathbf{r}, \mathbf{\Omega}, t) d\Omega dt \right\} \quad . \tag{25}$$

Then, using Eqs. (24) and (25), the average value of U_r over the time step is given by

$$\tilde{U}_r = \frac{1}{1+\alpha\beta_n c\sigma_n \Delta t_n} U_r(T_n) + \frac{\alpha\beta_n\sigma_n}{1+\alpha\beta_n c\sigma_n \Delta t_n} \int_{t_n}^{t_{n+1}} \int I(\mathbf{r}, \mathbf{\Omega}, t) d\Omega dt \quad . \tag{26}$$

The following approximation for U_r within the time step is consistent with Eq. (26) :

$$U_r(T) = U_r(\mathbf{r}, t) \approx \frac{1}{1+\alpha\beta_n c\sigma_n \Delta t_n} U_r(T_n) + \frac{\alpha\beta_n\sigma_n \Delta t_n}{1+\alpha\beta_n c\sigma_n \Delta t_n} \int I(\mathbf{r}, \mathbf{\Omega}, t) d\Omega \quad . \tag{27}$$

Using Eq. (27), we can write the transport equation for the Fleck-Cummings method. Defining the Fleck factor as

$$f_n = \frac{1}{1+\alpha\beta_n c\sigma_n \Delta t_n} \quad , \tag{28}$$

and approximating U_r by Eq. (27), Eq. (20) becomes

$$\frac{1}{c}\frac{\partial I}{\partial t} + \mathbf{\Omega} \cdot \nabla I + \sigma_n I = \frac{1}{4\pi}\sigma_n (1-f_n) \int I(\mathbf{r}, \mathbf{\Omega}', t) d\Omega' + \frac{1}{4\pi}\sigma_n f_n c U_r(T_n) \quad . \tag{29}$$

Eq. (29) is a standard, linear transport equation which can be solved using a Monte Carlo simulation. To approximate the absorption-reemission process, the method adds an isotropic scattering term (representing photons absorbed and reemitted within the time step),

$$\frac{1}{4\pi}\sigma_n (1-f_n) \int I(\mathbf{r}, \mathbf{\Omega}', t) d\Omega' \quad , \tag{30}$$

and a source term (representing photons absorbed in previous time steps and reemitted during the current step),

$$\frac{1}{4\pi}\sigma_n f_n c U_r(T_n) \quad . \tag{31}$$

To update the material energy density, we approximate U_r in Eq. (22) by Eq. (27). This yields

$$U_m(T_{n+1}) = U_m(T_n) + \sigma_n f_n \int_{t_n}^{t_{n+1}} \int I(\mathbf{r},\mathbf{\Omega},t) d\Omega dt - c\sigma_n f_n \Delta t_n U_r(T_n) \quad . \tag{32}$$

The end of time-step temperature T_{n+1} can be calculated by solving Eq. (4).

3.2. The Carter-Forest Method

To derive the Carter-Forest Method [2], we solve Eq. (21) exactly for $U_r(T) = U_r(\mathbf{r},t)$ within the time step:

$$U_r(T) = U_r(T_n) e^{-c\sigma_n\beta_n(t-t_n)} + \int_{t_n}^{t} \int \sigma_n \beta_n e^{-c\sigma_n\beta_n(t-t')} I(\mathbf{r},\mathbf{\Omega},t') d\Omega dt' \quad . \tag{33}$$

Eq. (33) represents the approximation to U_r in the Carter-Forest method. We note that this estimate for U_r is not exact, since Eqs. (18) and (19) are used to approximate σ and β.

Substituting Eq. (33) into Eq. (20) yields the transport equation for the Carter-Forest method:

$$\frac{1}{c}\frac{\partial I}{\partial t} + \mathbf{\Omega}\cdot\nabla I + \sigma_n I = \frac{1}{4\pi} c\sigma_n \left[U_r(T_n) e^{-c\sigma_n\beta_n(t-t_n)} + \int_{t_n}^{t} \int \sigma_n \beta_n e^{-c\sigma_n\beta_n(t-t')} I(\mathbf{r},\mathbf{\Omega}',t') d\Omega' dt' \right] \quad . \tag{34}$$

In Eq. (34), we have approximated the absorption-reemission by including a time-dependent scattering term (representing photons absorbed and reemitted during the time step),

$$\frac{1}{4\pi} \int_{t_n}^{t} \int c\sigma_n\beta_n e^{-c\sigma_n\beta_n(t-t')} \sigma_n I(\mathbf{r},\mathbf{\Omega}',t') d\Omega' dt' \quad , \tag{35}$$

and a time-dependent source term (representing photons absorbed in previous time steps and emitted during the current step),

$$\frac{1}{4\pi} c\sigma_n U_r(T_n) e^{-c\sigma_n\beta_n(t-t_n)} \quad . \tag{36}$$

Eq. (35) represents a scattering process in which photons are absorbed, then reemitted at a later time isotropically. The probability distribution function for the reemission time is

$$c\sigma_n\beta_n e^{-c\sigma_n\beta_n(t-t')} \quad , \tag{37}$$

where t' is the absorption time and t is the reemission time. In standard implementations of the Carter-Forest method, photons that would be reemitted past the end of the time step are considered absorbed and added to the material energy.

To update the material energy density, Eq. (33) is substituted into Eq. (22). This yields

$$U_m(T_{n+1}) = U_m(T_n) + \int_{t_n}^{t_{n+1}} \int \sigma_n e^{-c\sigma_n\beta_n(t_{n+1}-t)} I(\mathbf{r},\mathbf{\Omega},t) d\Omega dt - \frac{U_r(T_n)}{\beta_n}(1 - e^{-c\sigma_n\beta_n\Delta t_n}) \quad . \tag{38}$$

As with the Fleck-Cummings method, Eq. (4) can be use to solve for the end of time-step temperature.

4. MAXIMUM PRINCIPLE FOR THE CARTER-FOREST METHOD

We now derive a maximum principle for the Carter-Forest method using a technique similar to that of Larsen and Mercier's [5]. For $T_L < T < T_U$, we define

$$\gamma(T) = a \max \left[\frac{T^4 - T_L^4}{U_m(T) - U_m(T_L)} \ , \ \frac{T_U^4 - T^4}{U_m(T_U) - U_m(T)} \right] \quad . \tag{39}$$

Our maximum principle now takes the following form:

Maximum Principle for the Carter-Forest Method. Let $0 \leq T_L < T_U$ be fixed constants, and let I_i, T_i, and I_b satisfy Eqs. (8)-(10). Also, let

$$\sup_{T_L<T<T_U} \frac{\gamma(T)}{\beta(T)} \leq 1 \quad . \tag{40}$$

Alternatively, for all n, let

$$\Delta t_n \leq \inf_{T_L<T<T_U} \frac{1}{c\sigma(T)\beta(T)} \ln \left[\frac{\gamma(T)/\beta(T)}{\gamma(T)/\beta(T) - 1} \right] \quad . \tag{41}$$

Then, if I and T_n denote the Carter-Forest radiation intensity and material temperature, we have for all $t \geq 0$,

$$\frac{1}{4\pi} a c T_L^4 \leq I(\mathbf{r}, \mathbf{\Omega}, t) \leq \frac{1}{4\pi} a c T_U^4 \quad , \tag{42}$$

and for all integers $n \geq 0$,

$$T_L \leq T_n(\mathbf{r}) \leq T_U \quad . \tag{43}$$

Proof. The proof is by induction on time step n. The induction hypothesis is that I_n and T_n satisfy Eqs. (8) and (9) (this is true for $n = 0$), and I_b satisfies Eq. (10) (this is true for all n). Then, if Eqs. (40) or (41) are satisfied, we show that

$$\frac{1}{4\pi} a c T_L^4 \leq I(\mathbf{r}, \mathbf{\Omega}, t) \leq \frac{1}{4\pi} a c T_U^4 \quad , \quad t_n \leq t \leq t_{n+1} \quad , \tag{44}$$

and

$$T_L \leq T_{n+1}(\mathbf{r}) \leq T_U \quad . \tag{45}$$

First, we prove Eq. (44). We begin by defining

$$\psi(\mathbf{r}, \mathbf{\Omega}, t) = \frac{1}{4\pi} a c T_U^4 - I(\mathbf{r}, \mathbf{\Omega}, t) \quad . \tag{46}$$

We wish to show that $\psi \geq 0$. Introducing Eq. (46) into Eq. (34), we obtain

$$\frac{1}{c} \frac{\partial \psi}{\partial t} + \mathbf{\Omega} \cdot \nabla \psi + \sigma_n \psi - \frac{1}{4\pi} \int_{t_n}^{t} \int c \sigma_n \beta_n e^{-c\sigma_n \beta_n (t-t')} \sigma_n \psi(\mathbf{r}, \mathbf{\Omega}', t') d\Omega' dt' = Q \quad , \tag{47}$$

where

$$Q = \frac{1}{4\pi} \sigma_n c U_r(T_U) - \frac{1}{4\pi} \sigma_n c U_r(T_n) e^{-c\sigma_n \beta_n (t-t_n)} - \frac{1}{4\pi} \int_{t_n}^{t} \int c \sigma_n \beta_n e^{-c\sigma_n \beta_n (t-t')} \frac{1}{4\pi} \sigma_n c U_r(T_U) d\Omega' dt' \quad . \tag{48}$$

By the induction hypothesis and Eq. (46), ψ has non-negative initial and boundary values. Thus, since ψ satisfies a standard linear transport problem (with time-dependent scattering), ψ is non-negative if the source term is non-negative [3]. Simplifying Eq. (48) and employing Eq. (13), we have

$$Q = \frac{1}{4\pi}\sigma_n c e^{-c\sigma_n\beta_n(t-t_n)} a(T_U^4 - T_n^4) \geq 0 \quad . \tag{49}$$

Thus, Q is non-negative regardless of the time-step size, $0 \leq \psi$, and $I \leq \frac{1}{4\pi} c a T_U^4$ for $t_n \leq t \leq t_{n+1}$. In a similar manner, one can show that $\frac{1}{4\pi} c a T_L^4 \leq I$ for $t_n \leq t \leq t_{n+1}$. This completes the proof of Eq. (44).

To prove Eq. (45), we instead verify the equivalent inequalities

$$U_m(T_L) \leq U_m(T_{n+1}) \leq U_m(T_U) \quad . \tag{50}$$

Using Eq. (38), Eq. (50) can be written as

$$\int_{t_n}^{t_{n+1}} \int \sigma_n e^{-c\sigma_n\beta_n(t_{n+1}-t)} I(\mathbf{r},\mathbf{\Omega},t) d\Omega dt - \frac{U_r(T_n)}{\beta_n}(1 - e^{-c\sigma_n\beta_n\Delta t_n}) \leq U_m(T_U) - U_m(T_n) \quad , \tag{51}$$

$$\frac{U_r(T_n)}{\beta_n}(1 - e^{-c\sigma_n\beta_n\Delta t_n}) - \int_{t_n}^{t_{n+1}} \int \sigma_n e^{-c\sigma_n\beta_n(t_{n+1}-t)} I(\mathbf{r},\mathbf{\Omega},t) d\Omega dt \leq U_m(T_n) - U_m(T_L) \quad . \tag{52}$$

Using Eqs. (44) and (13), Eqs. (51) and (52) are satisfied if

$$\frac{a}{\beta_n}\left[\frac{T_U^4 - T_n^4}{U_m(T_U) - U_m(T_n)}\right](1 - e^{-c\sigma_n\beta_n\Delta t_n}) \leq 1 \quad , \tag{53}$$

$$\frac{a}{\beta_n}\left[\frac{T_n^4 - T_L^4}{U_m(T_n) - U_m(T_L)}\right](1 - e^{-c\sigma_n\beta_n\Delta t_n}) \leq 1 \quad . \tag{54}$$

Eqs. (53) and (54) can be combined into a single inequality using Eq. (39):

$$\frac{\gamma(T_n)}{\beta_n}(1 - e^{-c\sigma_n\beta_n\Delta t_n}) \leq 1 \quad . \tag{55}$$

We note that if Eq. (40) is satisfied, Eq. (55) holds for all Δt_n. Otherwise we rewrite Eq. (55) as

$$\Delta t_n \leq \frac{1}{c\sigma_n\beta_n} \ln\left[\frac{\gamma(T_n)/\beta_n}{\gamma(T_n)/\beta_n - 1}\right] \quad , \tag{56}$$

which holds if Eq. (41) is satisfied.

The conditions that guarantee that the Carter-Forest method satisfies the maximum principle, Eqs. (40) and (41), are sufficient (not necessary) conditions. Thus, although the maximum principle is guaranteed to be satisfied if Eqs. (40) and (41) are satisfied, the maximum principle may not be violated if Eqs. (40) and (41) are not satisfied. This phenomenon is commonly observed in practice, and is a limitation of employing the maximum principle to quantify stability.

5. COMPARISON TO THE FLECK-CUMMINGS METHOD

Larsen and Mercier have derived a maximum principle for the Fleck-Cummings method using a similar technique [5]. In their analysis, they showed that the Fleck-Cummings method satisfies the maximum principle if

$$\sup_{T_L<T<T_U} \frac{\gamma(T)}{\beta(T)} \leq \alpha \quad , \tag{57}$$

or, for all $n \geq 0$,

$$\Delta t_n \leq \inf_{T_L<T<T_U} \frac{1}{c\sigma(T)\beta(T)\left[\gamma(T)/\beta(T)-\alpha\right]} \quad . \tag{58}$$

We now compare the Fleck-Cummings and Carter-Forest methods for the "implicit" Fleck-Cummings method ($\alpha = 1$) in the case when Eqs. (40) and (57) are not satisfied. Using

$$\ln x \leq x - 1 \quad , \quad x \geq 1 \quad , \tag{59}$$

we note that

$$\frac{1}{c\sigma(T)\beta(T)} \ln\left[\frac{\gamma(T)/\beta(T)}{\gamma(T)/\beta(T)-1}\right] \leq \frac{1}{c\sigma(T)\beta(T)\left[\gamma(T)/\beta(T)-1\right]} \quad . \tag{60}$$

Thus, Eqs. (41) and (58) can be compared by

$$\inf_{T_L<T<T_U} \frac{1}{c\sigma(T)\beta(T)} \ln\left[\frac{\gamma(T)/\beta(T)}{\gamma(T)/\beta(T)-1}\right] \leq \inf_{T_L<T<T_U} \frac{1}{c\sigma(T)\beta(T)\left[\gamma(T)/\beta(T)-1\right]} \quad . \tag{61}$$

Thus, the Fleck-Cummings method is guaranteed to satisfy the maximum principle for a larger time-step size than the Carter-Forest method, when $\alpha = 1$.

If the heat capacity is proportional to T^3, as in Su and Olson's "linear" problem [8], then, using Eqs. (4), (15), and (39), $\gamma/\beta = 1$ for all temperatures and β is a constant. In this case, Eqs. (40) and (57) (for $\alpha = 1$) are satisfied, and both the Carter-Forest and Fleck-Cummings methods satisfy the maximum principle regardless of the time-step size. In more general problems, however, the heat capacity is not proportional to T^3 and β varies as a function of temperature. Thus, the explicit approximation of β in Eq. (21) seems to be a dominant cause in violations of the maximum principle. An improved method, which aims to suppress violations of the maximum principle, must employ a more accurate representation of β over the time step. Somehow, β must be treated in an implicit manner, rather than using a beginning of time-step value for the temperature.

6. NUMERICAL RESULTS

We now present the results from two radiative transfer problems in which Planckian surface sources are incident on the left and right boundaries of a 4 cm slab with an initial temperature of T_i=0.001 keV or 0.6 keV. In these problems, the material has a constant opacity of 1.0 cm^{-1} and a constant heat capacity of 0.001 jk/cm^3-keV (1 jk=1 jerk=10^9 Joules). The temperature at the left boundary is 1 keV, while the temperature on the right boundary is identical to the initial temperature. These two problems were simulated with both the Carter-Forest and Fleck-Cummings methods using a 0.1 cm spatial mesh and 10^8 particles per jerk. In calculations employing the Fleck-Cummings method, α was set equal to unity.

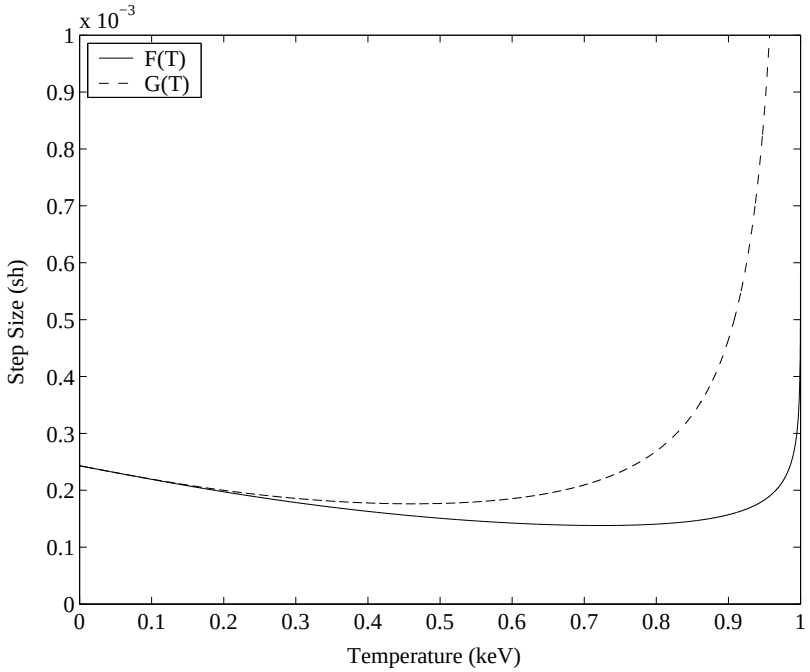

Figure 1. Maximum Step Size for Carter-Forest and Fleck-Cummings Methods

Since we consider a constant heat capacity, Eq. (39) now takes the form

$$\gamma(T) = \frac{a}{C_v}\frac{T_U^4 - T^4}{T_U - T} \quad . \tag{62}$$

Also, since Eqs. (40) and (57) are not satisfied, we define

$$F(T) = \frac{1}{c\sigma(T)\beta(T)} \ln\left[\frac{\gamma(T)/\beta(T)}{\gamma(T)/\beta(T) - 1}\right] \quad , \tag{63}$$

and

$$G(T) = \frac{1}{c\sigma(T)\beta(T)\left[\gamma(T)/\beta(T) - \alpha\right]} \quad . \tag{64}$$

From Eqs. (41) and (58), the minimums of F and G over the range $T_L \leq T \leq T_U$ yield the maximum time-step size that guarantees the maximum principle is satisfied for the Carter-Forest and Fleck-Cummings methods, respectively. For the above problems, T_U=1.0 keV and $T_L = T_i$.

Figure 1 gives a plot of Eqs. (63) and (64) for T_U=1.0 keV. For T_L near zero (i.e. radiation incident on a initially cold slab) the minima of G and F over $T_L \leq T \leq T_U$ are nearly identical. In these types of problems, the Carter-Forest and Fleck-Cummings methods should satisfy the maximum principle for nearly the same maximum time-step size. However, as T_L approaches T_U, the minimum of G is much larger than the minimum of F. In this regime, we would expect the Fleck-Cummings method to satisfy the maximum principle for a larger time step than the Carter-Forest method.

We now examine the problem in which T_i=0.001 keV. From Figure 1, the maximum principle is guaranteed to be satisfied by both methods if the time-step size is chosen such that $\Delta t \lesssim 2 \times 10^{-4}$sh (1 sh=1 shake=$10^{-8}$ seconds), with the Carter-Forest method requiring a slightly smaller time step than the

Fleck-Cummings method. From our numerical calculations, however, we found that the maximum principle is satisfied by both methods for $\Delta t < 1 \times 10^{-3}$sh. Thus, the theoretical bound for Δt is overly conservative. However, we note that Figure 1 predicted that both Monte Carlo methods would require approximately the same time-step size to satisfy the maximum principle, which was observed in our calculations.

In Figures 2 and 3, we demonstrate a violation of the maximum principle using the Fleck-Cummings method (the Carter-Forest method gave similar results). In Figure 2, the average material temperature in each cell is plotted for $t = \Delta t$ =0.005 sh. In Figure 3, the average material temperature in the leftmost cell (i.e. $x = \Delta x/2$ =0.05 cm) is plotted as a function of time. From these plots it is obvious that the maximum principle is violated (the temperature in the first cell is nearly 8 keV at the end of the first time step). The magnitude by which the maximum principle is violated decreases for successive time steps, until the material temperature is consistent with the maximum principle. Physically, radiation is incident on an initially cold slab. As radiation is absorbed, the slab material energy and temperature increase, and the material emits photons. However, since Eqs. (20) and (21) contain explicit approximations based on the beginning of time-step temperature, the emission rate of photons does not increase at the correct rate with respect to the material energy and temperature. At the end of the time step, the net energy absorbed by the material is too large, and an unphysical temperature is calculated. This phenomenon causes violations of the maximum principle.

Finally, we examine the case of an initial temperature of 0.6 keV. For this problem, Figure 1 predicts approximately the same theoretical bound on Δt as for the T_i=0.001 keV problem. The cell-average material temperature for $t = \Delta t$ =0.002 sh is plotted in Figure 4, and the cell-average material temperature in the leftmost cell is plotted in Figure 5 as a function of time. In this problem we note that the Carter-Forest method violates the maximum principle for the first cell at the end of the first time step, while the Fleck-Cummings method does not. However, both methods overestimate the temperature in the first cell at the end of the first time step. At later times, the temperature in the first cell decreases, and both methods satisfy the maximum principle. For smaller time steps, both Monte Carlo methods satisfy the maximum principle. Again, the theoretical bound on the time step is too conservative. However, our theory predicts that as T_L approaches T_U, the Fleck-Cummings method would satisfy the maximum principle for a larger time step than the Carter-Forest method.

7. CONCLUSIONS

In this paper, we have derived theoretical constraints on the time-step size for the Carter-Forest method that ensure solutions generated by this method satisfy a maximum principle. In addition, we have compared our analysis to a similar analysis of the Fleck-Cummings method, and have shown that the Fleck-Cummings method is guaranteed to satisfy the maximum principle for larger time steps than the Carter-Forest method.

With a set of example problems, we have demonstrated that the theoretical constraints on the time-step size are overly conservative. However, our numerical results agree with our theory in two respects. First, if the upper and lower temperature bounds are far apart, both Monte Carlo methods violate the maximum principle for the same time-step size. In addition, for upper and lower temperature bounds near each other, the Fleck-Cummings method satisfies the maximum principle for a larger time-step than the Carter-Forest method.

The first problem presented in our numerical results is representative of a large class of radiative transfer

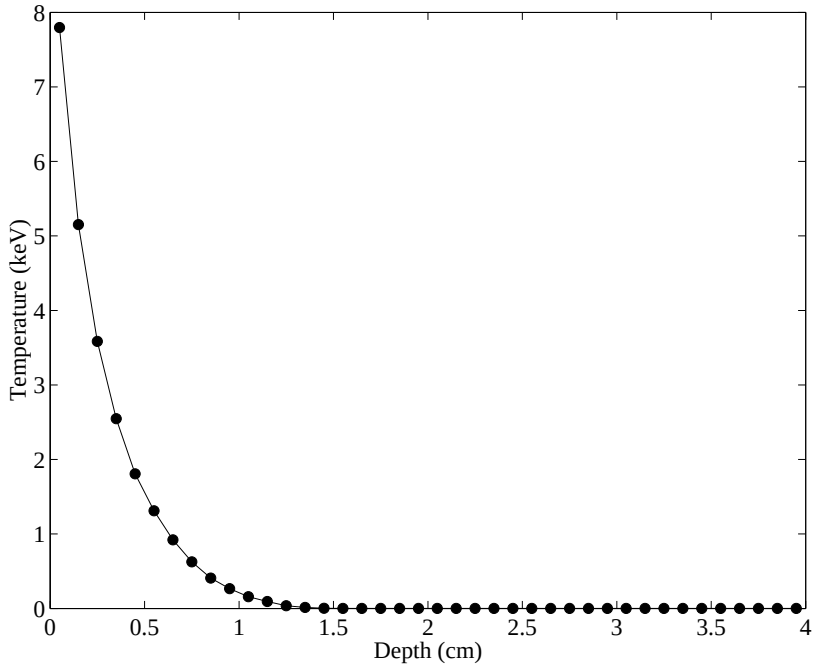

Figure 2. Material Temperature at t=Δt=0.005 sh (T_i=0.001 keV)

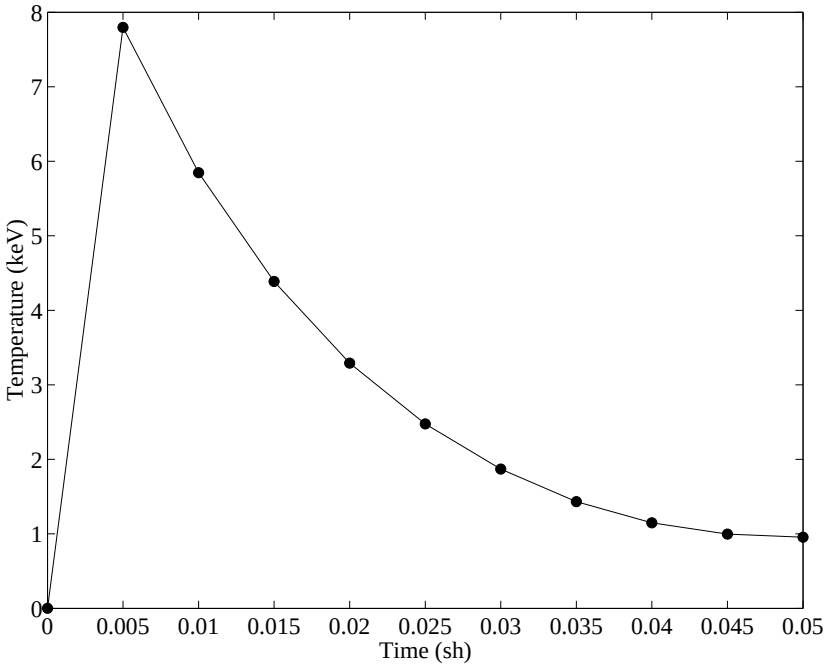

Figure 3. Material Temperature at x=Δx/2=0.05 cm (T_i=0.001 keV)

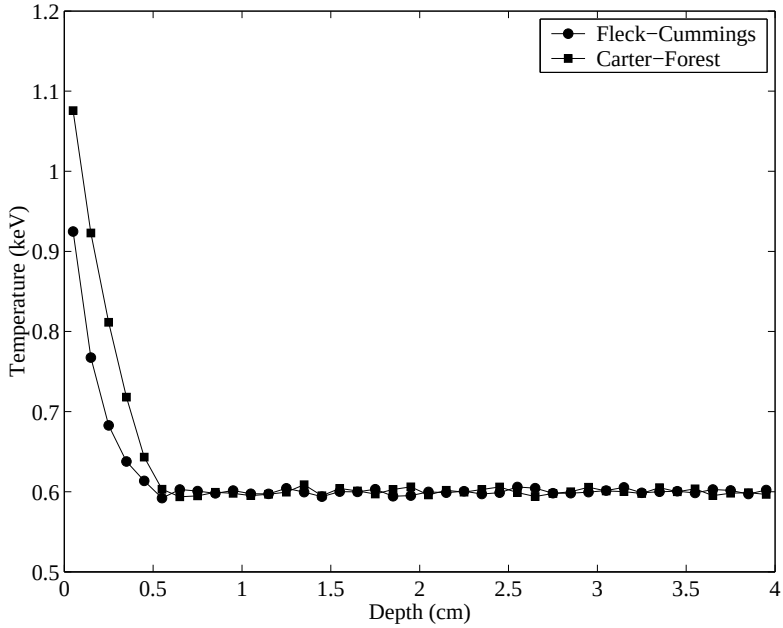

Figure 4. Material Temperature at t=Δt=0.002 sh (T_i=0.6 keV)

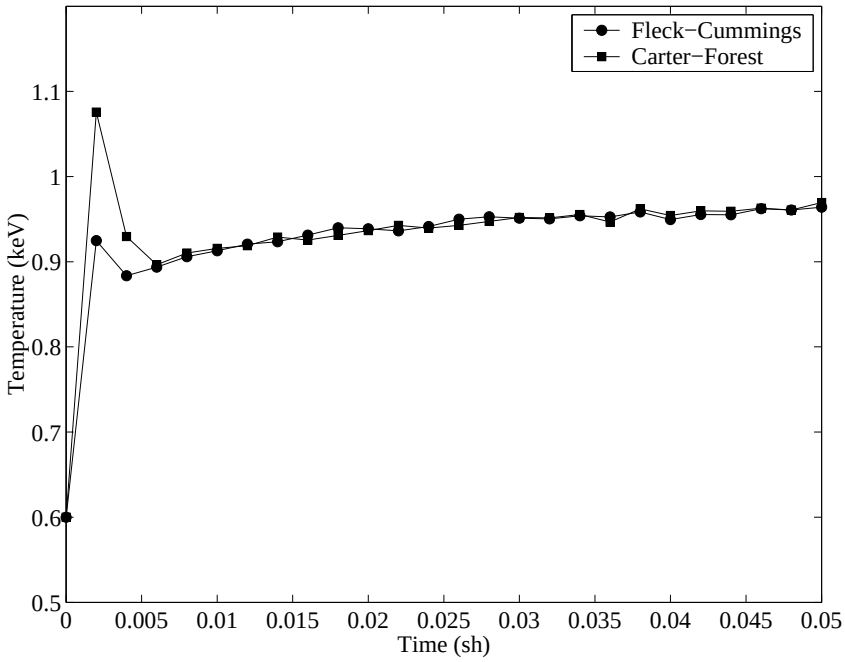

Figure 5. Material Temperature at x=Δx/2=0.05 cm (T_i=0.6 keV)

problems, in which "hot" radiation is incident on an initially "cold" medium. From our theoretical analysis and numerical results, we would expect both the Carter-Forest and Fleck-Cummings methods to behave in a similar manner for this class of problems. Thus, for this group of problems, there may be no advantage in using one method over the other. The second problem presented in our numerical results is representative of a smaller class of problems, in which an initially "warm" medium is perturbed by an increase in the incident radiation intensity. From our results it would seem that the Fleck-Cummings method has an advantage over the Carter-Forest method, in that larger time steps may be employed without violating the maximum principle.

Although our theoretical results are too conservative, this paper serves as a comparison of both Monte Carlo methods with respect to stability. In future work we plan on examining frequency-dependent radiative transfer problems.

ACKNOWLEDGMENTS

We wish to thank Todd Urbatsch and Tom Evans for their helpful comments. The work of the first author (JDD) was performed under U.S. Government contract W-7405-ENG-36 for Los Alamos National Laboratory, which is operated by the University of California for the U.S. Department of Energy.

REFERENCES

[1] E.S. Andreev, M.Y. Kozmanov, and E.B. Rachilov, "The Maximum Principle for a System of Equations of Energy and Non-stationary Radiation Transfer," *U.S.S.R. Comput. Math. Math. Phys.*, **23**, pp. 104-109 (1983).

[2] L.L. Carter and C.A. Forest, "Nonlinear Radiation Transport Simulation with an Implicit Monte Carlo Method," LA-5038, Los Alamos National Laboratory (1973).

[3] K.M. Case and P.F. Zweifel, *Linear Transport Theory*, Addison-Wesley, Reading, Massachusetts (1967).

[4] J.A. Fleck, Jr. and J.D. Cummings, "An Implicit Monte Carlo Scheme for Calculating Time and Frequency Dependent Nonlinear Radiation Transport," *J. Comp. Phys.*, **8**, pp. 313-342 (1971).

[5] E.W. Larsen and B. Mercier, "Analysis of a Monte Carlo Method for Nonlinear Radiative Transfer," *J. Comp. Phys.*, **71**, pp. 50-64 (1987).

[6] B. Mercier, "Application of Accretive Operators Theory to the Radiative Transfer Equations," *SIAM J. Math. Anal.*, **18**, pp. 393-408 (1987).

[7] G.C. Pomraning, *The Equations of Radiation Hydrodynamics*, Pergamon, Oxford, United Kingdom (1973).

[8] B. Su and G.L. Olson, "An Analytical Benchmark for Non-Equilibrium Radiative Transfer in an Isotropically Scattering Medium," *Ann. Nucl. Energy*, **24**, pp. 1035-1055 (1997).